UNIVERSIDADE DE SÃO PAULO

INSTITUTO DE FÍSICA
CAIXA POSTAL 20516
01498 - SÃO PAULO - SP
BRASIL

PUBLICAÇÕES

IFUSP/P-537

MIRNOV OSCILLATIONS IN A SMALL TOKAMAK

by

I.H. Tan, I.L. Caldas, I.C. Nascimento, R.P. da Silva, E.K. Sanada, and R. Bruha

Instituto de Física, Universidade de São Paulo

Julho/1985

MIRNOV OSCILLATIONS IN A SMALL TOKAMAK

I.H. Tan, I.L. Caldas, I.C. Nascimento, R.P. da Silva,
E.K. Sanada, and R. Bruha

Instituto de Física, Universidade de São Paulo,
C.P. 20516, 01498 São Paulo, SP, Brasil

ABSTRACT

This paper presents the results obtained in the small tokamak TBR-1, concerning Mirnov oscillations. The phase correlation method using 20 magnetic coils was applied to determine the poloidal and toroidal mode numbers. The main modes detected had m=2 and m=3, both with n=1, for q_ℓ (the safety factor at the limiter) varying from 4 to 7. The amplitudes and frequencies were measured, and a discussion is made about the TBR-1 confinement and stability conditions.

INTRODUCTION

Low frequency oscillations ($f \leq 100$ kHz) of the poloidal magnetic field are normally observed in tokamaks [1,2]. These oscillations, usually called Mirnov oscillations, have spatial helical structures of the form $\cos(m\theta - n\phi)$, where θ and ϕ are respectively the poloidal and toroidal angles and the integers m and n are the poloidal and toroidal mode numbers. The Mirnov oscillations are actually the external manifestation of the rotation of helical magnetic islands caused by resistive tearing modes [2]. When Mirnov oscillations are present, the confinement deteriorates and, in the worst cases, a violent and very fast instability, called disruptive instability, terminates the plasma [3,4]. This violent loss of confinement is not yet well understood, but it is almost always preceeded by growing Mirnov oscillations [5]. The presently accepted interpretation is that the corresponding magnetic islands grow to such amplitudes that they can interact with the limiter or with other islands of different helicities causing the loss of confinement [4].

In this paper we present the main characteristics of the Mirnov oscillations measured in the small tokamak TBR-1 [6] of the Physics Institute at the University of São Paulo. The poloidal magnetic field oscillations were detected by 20 magnetic coils conveniently distributed along the torus [7], so that the mode numbers m and n could be determined using a phase correlation method [8]. The amplitudes and frequencies were also obtained for different equilibria. The experimental results were compared with theoretical estimatives of these parameters based on TBR-1 characteristics.

EXPERIMENTAL SET-UP

TBR is a small air-core low beta tokamak ($\beta \sim 5 \times 10^{-4}$) with no conducting shell. The equilibrium is maintained by an externally applied vertical field. The main parameters of the machine and the plasma parameters for the experiment reported here are the following:

major radius	0.30 m ,
minor radius	0.11 m ,
radius at limiter	0.08 m ,
toroidal magnetic field	(0.4 - 0.45) T ,
plasma current	(6 - 12) kA ,
electron temperature	$\gtrsim$ 30 eV ,
density (hydrogen)	(5 - 10) 10^{19} m^{-3} ,
discharge duration	(2 - 6) ms .

The poloidal magnetic field oscillations were measured by 16 coils equally spaced in the poloidal direction at a fixed toroidal position and 4 coils separated by 90° in the toroidal direction at a fixed poloidal position. The coils were placed inside the stainless steel vacuum vessel to avoid attenuation of the MHD oscillations. For the 3 mm thickness of the vacuum vessel of TBR-1, the attenuation is about 80% for a typical frequency of 50 kHz of the MHD oscillations.

The poloidal coils were enclosed in curved stainless steel tubes, 0,2 mm thick (corresponding to an attenuation of only 15% in 50 kHz), placed inside the vessel in the shadow of the limiter (fig. 1a). During discharge cleaning operation, the temperature inside the tubes can reach values of the order of 200°C. In order to avoid melting of the wire insulation,

the coils were cooled by forced air circulation inside the tubes (fig. 1b). The coils were calibrated in a standard Helmholtz coil. The effective area was found to be $(18.6 \pm 1.0) \times 10^{-4}$ m^2.

The toroidal coils with an effective area of $(7.7 \pm 1.0) \times 10^{-4}$ m^2 were inserted inside the vessel using ceramic tubes (fig. 2).

The coil signals were recorded in the memory modules of two eight channel ADC modules. After the shot the signals were displayed in an oscilloscope and photographed. In discharges with strong MHD activity (usually with high plasma currents), the signals had to be attenuated through differential amplifiers with a 0.1 gain to prevent the signal amplitudes from exceeding the 0.25 V ADC limit. In these cases the low frequency noise caused by the raising of the tokamak magnetic fields were also attenuated by high-pass filters (3 dB at 2 kHz).

The usual phase correlation method was used to analyze the data. From the relative phases of the 16 poloidal coil signals, $\tilde{B}_\theta = \tilde{B}_\theta(\theta)$ curves were traced at different times and Fourier analyzed in θ to determine the present poloidal mode numbers (m). Similarly, the toroidal mode number (n) was determined by the relative phases of the 4 toroidal coil signals. In all cases this mode number was found to be n=1.

The experiments were performed with the working parameters already mentioned. Because of the limited capacity of the data acquisition system, the density and the electron temperature were not measured. Their values were estimated from the results of previous experiments [9,10]. The basic plasma parameters measured together with the MHD activity were the loop voltage, the plasma current, the horizontal displacement of the plasma column [11] and the hard X-rays signals

(measured with a NaI crystal coupled to a photomultiplier and an active integrator).

The MHD oscillations reported here were detected after an equilibrium state was set up. Fig. 3a shows typical oscillations detected by some of the poloidal coils. The main frequency is about 37 kHz (the oscillations were not Fourier analyzed in time). It can be seen in this figure that the oscillation amplitudes are not symmetric in θ. Fig. 4 is a plot of the typical dependence of the oscillation amplitudes on the poloidal position (θ) of the coils. The rate $\tilde{B}_{\theta max}/\tilde{B}_{\theta min}$ is in general around 6. This asymmetry indicates that the magnetic islands which originate the measured perturbations were displaced downward and to the outside of the geometrical axis of the torus. In fact the entire plasma column was displaced to the outside and to the bottom of the tokamak as indicated by the horizontal and vertical position coils. The outward displacement could not be avoided by increasing the external vertical field since in this case equilibrium would not be obtained.

The relative phases of the coil signals were obtained tracing $\tilde{B}_\theta = \tilde{B}_\theta(\theta)$ curves at different times (fig. 3b). $\tilde{B}_\theta(\theta)$, the relative amplitude of the oscillation, was normalized from -1 to +1, to prevent distortions caused by the asymmetry. Fig. 3c shows the Fourier spectra of these curves, indicating in this case a dominant m=3 mode. The poloidal structure of the modes can also be visualized by the polar graphs of the $\tilde{B}_\theta(\theta)$ curves (fig. 3d).

RESULTS

The results obtained showed that there were basically two types of discharge in TBR-1.

The first type were the discharges with low plasma currents (6 kA to 9 kA), which exhibit low MHD activity. The fluctuation levels $\tilde{B}_\theta/B_\theta$ (where $\tilde{B}_\theta$ is the average of the 16 amplitudes) is less than 1%. The discharge durations were usually about 6 ms. However, the MHD activity ceased after 2 ms, when hard X-rays signals showed the appearance of runaway electrons, probably due to the decreasing of plasma density [9]. In this experiment no gas puffing was used. Fig. 5 shows a typical low current discharge. The dominant modes detected had m=2 and m=3, always with n=1.

The second type of discharge had high plasma currents (10 kA to 12 kA) and a much stronger MHD activity. For this type of discharge the equilibrium was difficult to obtain (as it is pointed out at the end of this section). The fluctuation levels $\tilde{B}_\theta/B_\theta$ were between 1% and 2%. The discharge durations were about 2 ms and no runaway electrons were detected. Fig. 6 is an example of such a high current discharge. Dominant modes have m=2 and m=3, with n=1.

The fluctuation levels $\tilde{B}_\theta/B_\theta$ was the only oscillation parameter noticeably dependent on the plasma current intensity.

The main modes detected had poloidal numbers m=2 and m=3, always with n=1. Modes with m=4, n=1 were occasionally detected in low plasma currents. Tearing mode theory predicts that an m,n mode can only exist if the resonant surface with $q = m/n$ is within the plasma [12,13].

The q_ℓ independence of m/n (where q_ℓ is the safety factor at the limiter, which is directly related to the plasma current intensity) shows that the two types of discharge had probably different plasma profiles, so that magnetic surfaces with q=2 and q=3 were present in all discharges.

The oscillation frequencies varied in time and were usually between 30 kHz and 75 kHz. However, in low plasma currents higher frequency oscillations were sometimes detected ($f \sim 90$ kHz). The rotation frequencies f/m were between 10 kHz and 40 kHz, which is the same order of magnitude as the electron diamagnetic drift frequency. The modes also rotated in the direction of the electron diamagnetic drift. The drift frequency was roughly estimated as 15 kHz in TBR-1, although we still do not have information on the density and temperature profiles. Thus the radius of the resonant surface could not be properly determined. The temporal evolution of the rotation frequency is shown in fig. 7 for the discharge conditions indicated in fig. 6. The lowest point in fig. 7 corresponds to a dominant m=3 mode and the other two, to a dominant m=2 mode. This can be seen in fig. 6 where the poloidal structures of the oscillations at the times corresponding to those points are shown. The ratio f/m could not be determined in some time intervals during this discharge because none of the m=2 and m=3 modes detected were clearly dominant.

Fig. 8(a-b) shows the fluctuation levels $\tilde{B}_\theta/B_\theta$ of the m=2, n=1 and m=3, n=1 modes detected, as a function of the safety factor at the limiter (q_ℓ). In both cases there is a strong increase of $\tilde{B}_\theta/B_\theta$ as q_ℓ decreases from 7 to 4. This is the qualitatively expected behaviour according to non-linear tearing mode theory [14]. In fact, the oscillations

detected are believed to be due to the rotation of resistive magnetic islands because $q_\ell > m/n$ in all cases, implying that the condition $q_a > m/n$ is satisfied. The characteristic time for the growth of linear tearing modes is estimated to be of the order of 10^{-5} s for the conditions of TBR-1. This is much faster than the characteristic time of the observed oscillations, indicating that the detected modes were already in a non-linear saturated regime [14].

A common feature of most of the discharges was the absence of MHD oscillations during the raising of the plasma current. In this phase of the discharge, the observed oscillations did not show a well defined spatial or temporal structure. This could be explained by the fact that the amplitudes of the oscillations with large m (which should appear during the current rise when q_ℓ is also large) were small compared with the amplitude of turbulent magnetic oscillations [15]. Another possible explanation is that the rate of current rise could be small enough so that MHD oscillations would not exist [16]. In fact for most of the discharges with plasma currents greater than 10 kA, positive spikes on the loop voltage were observed during the current rise. These shots had a great predisposition to disrupt during this phase, and the equilibrium was difficult to obtain. This suggested the existence of a current rise MHD activity for these discharges, although they were not clearly observable in the coils. Since in this experience all shots had about the same current rise time, it seemed that there was a maximum rate of current rise ($\dot{I}$) for the discharges to evolve free of disruptions. This maximum was lower for higher plasma current intensities as it has been reported in ref. [16].

CONCLUSIONS

Without feedback control of the plasma position, equilibrium was obtained when the plasma column was displaced outwards. This behaviour seems to be in agreement with the observations made on Pulsator [17], where the plasma was less sensible to disruptive instabilities when it was slightly displaced outwards.

For the discharges with low plasma currents the MHD oscillations were not detected during the raising of the plasma current. For most of the discharges with plasma currents greater than 10 kA soft disruptions were observed during this phase and equilibrium was not obtained. This could be a consequence of the equal plasma current rise time for all the discharges [16].

The usual phase correlation method [8] was applied to determine the MHD modes present in the discharges of the TBR-1 tokamak. The oscillations were detected after an equilibrium state was set up. The main modes detected had $m=3$ and $m=2$, always with $n=1$. Simultaneous modes were detected. This could be partly interpreted as a consequence of the toroidal geometry, because a pure mode m would be expected to appear with side-band modes $m' = m \pm 1$. The modes rotated in the direction and roughly with the frequency of the electron diamagnetic drift. The dependence of the fluctuation levels $\tilde{B}_\theta/B_\theta$ on the safety factor at the limiter was determined, and it was in qualitative agreement with the expected behaviour of non-linear tearing modes [14]. The poloidal mode numbers usually varied in time, without any noticeable change of the safety factor at the limiter. This could be explained by changes in the plasma profiles [12,13].

ACKNOWLEDGEMENTS

We would like to thank Dr. R.M.O. Galvão for useful discussions and for reading the manuscript. Thanks are also due to Dr. W.C. Las for reading the manuscript. This work has been partially supported by FAPESP, FINEP, CNPq and CNEN.

REFERENCES

[1] S.V. Mirnov, Nucl. Fus. 9, 57 (1969).

[2] D.C. Robinson, Phil. Trans. R. Soc. Lond. A300, 525 (1981).

[3] F. Karger et al., Proc. 6th Int. Conf. Plasma Phys. Contr. Nucl. Fus. Res., Berchtesgaden 1976, IAEA-CN-35/A-7.

[4] Proc. IAEA Symp. Current Disruption in Toroidal Devices, Garching 1979, Report IPP 3/51 (1979).

[5] R.S. Granetz, Rev. Scient. Inst. 52, 1332 (1981).

[6] I.C. Nascimento et al., Proc. Spring College on Fus. Energy, ICTP, Trieste, Italy (1981), IAEA SMR-82, pg. 45 .

[7] I.H. Tan et al., Proc. Int. Conf. Plas. Phys., Lausanne 1984, P6-4.

[8] TFR Group, Nucl. Fus. 18, 647 (1978).

[9] R.S. Dallaqua et al., Il Nuovo Cimento 83B, 1 (1984).

[10] E.K. Sanada, Master's Degree Thesis, Physics Inst., Univ. of São Paulo, 1983.

[11] A.Y. Ueta, Master's Degree Thesis, Physics Inst., Univ. of São Paulo, 1985.

[12] H.P. Furth, P.H. Rutherford, H. Selberg, Phys. Fluids 16, 1054 (1973).

[13] H. Tasso, J.T. Virtamo, Plasma Physics 22, 1003 (1980).

[14] B. Carreras, B.V. Waddell, H.R. Hicks, Nucl. Fus. 19, 1423 (1979).

[15] R.A. Duperrex et al., Phys. Lett. 106A, 133 (1984).

[16] R.S. Granetz, I.H. Hutchinson, D.O. Overskei, Nucl. Fus. 19, 1587 (1979).

[17] O. Klüber, Report IPP III/14 (1974).

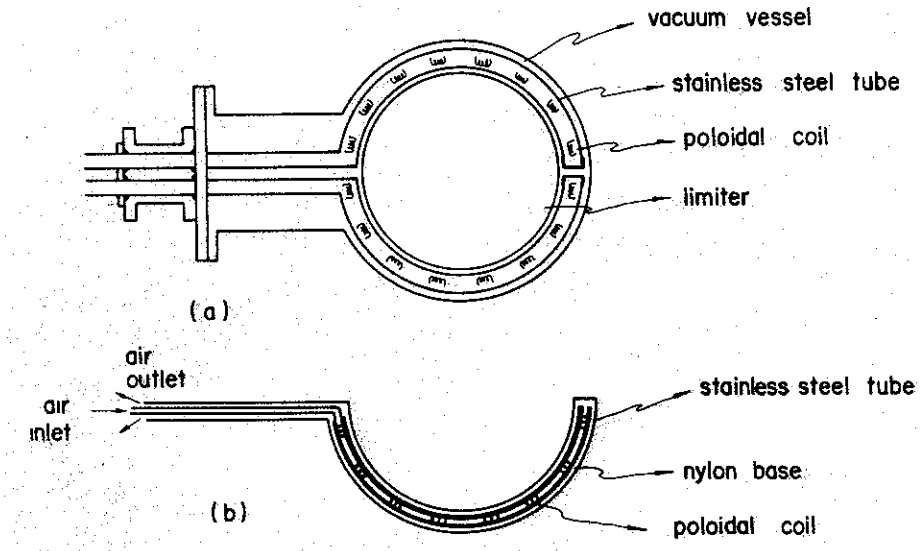

Fig. 1 - (a) Mechanical structure of poloidal coils.
(b) Cooling system of poloidal coils.

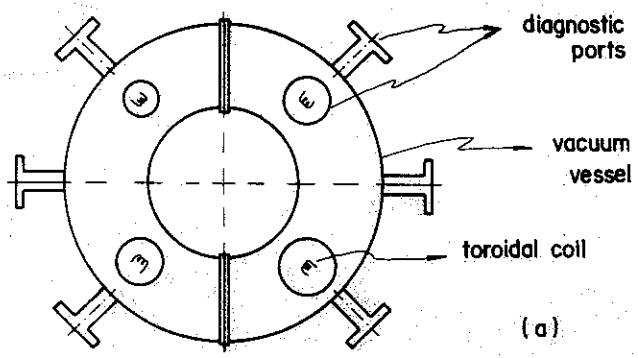

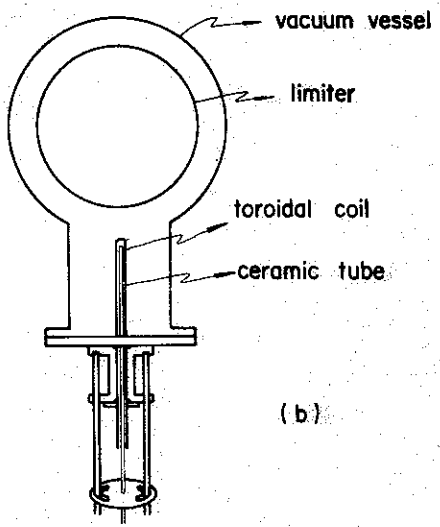

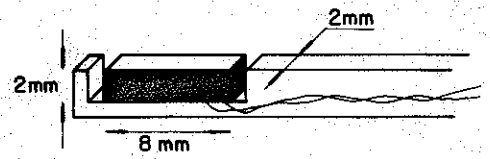

Fig. 2 - (a) Top view of TBR-1 showing the positions of the toroidal coils.

(b) Mechanical structure of toroidal coil.

(c) Dimensions of one toroidal coil.

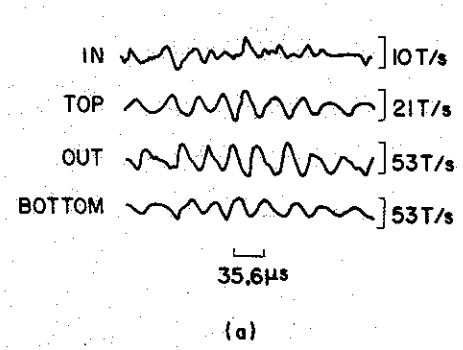

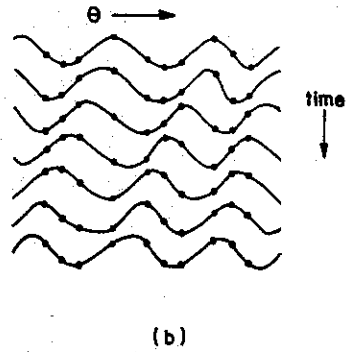

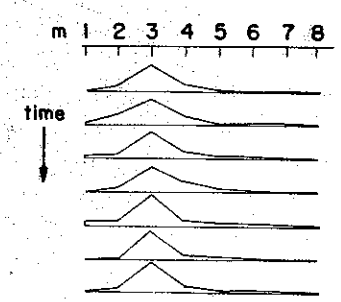

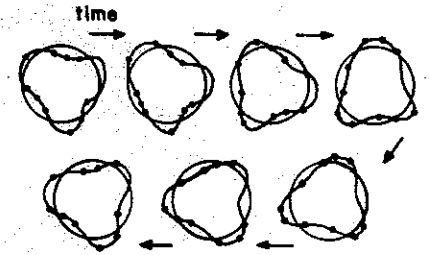

Fig. 3 - Determination of the poloidal numbers (m).

(a) Oscillations detected by four equally spaced poloidal coils.

(b) $\tilde{B}_\theta = \tilde{B}_\theta(\theta)$ curves (normalized from -1 to +1), showing the relative phases of the 16 poloidal coil signals at different times.

(c) Fourier spectra of the $\tilde{B}_\theta(\theta)$ curves showed in (b).

(d) Polar graphs of the $\tilde{B}_\theta(\theta)$ curves showed in (b).

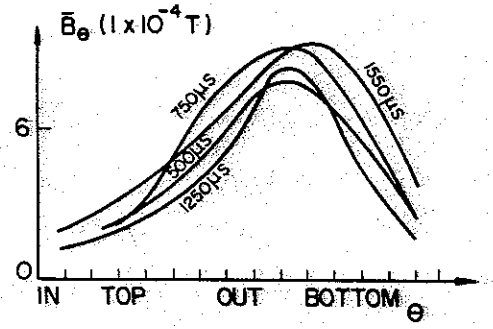

Fig. 4 - Oscillation amplitudes $\tilde{B}_\theta$ detected by the poloidal coils as a function of their angular position (θ). The data were taken at different times in the discharge shown in fig. 6.

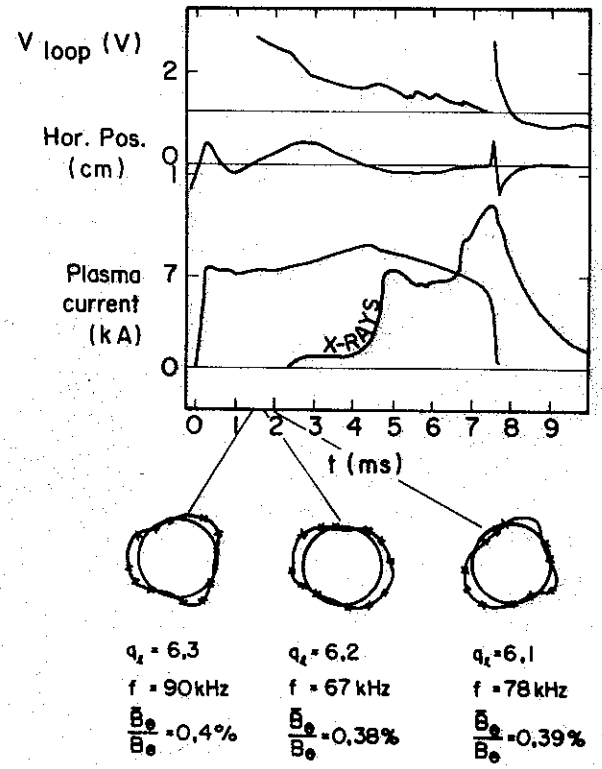

Fig. 5 - Temporal profiles of the loop voltage, horizontal plasma position and plasma current of a typical low current discharge. The poloidal structure of MHD modes are shown at three different times.

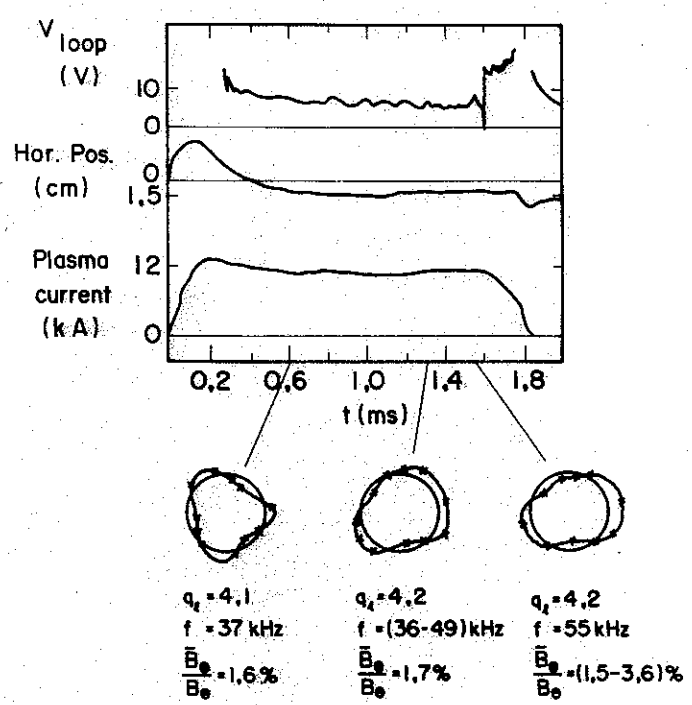

Fig. 6 - Temporal profiles of the loop voltage, horizontal plasma position and plasma current of a typical high current discharge. The poloidal structures of the MHD modes are shown at three different times.

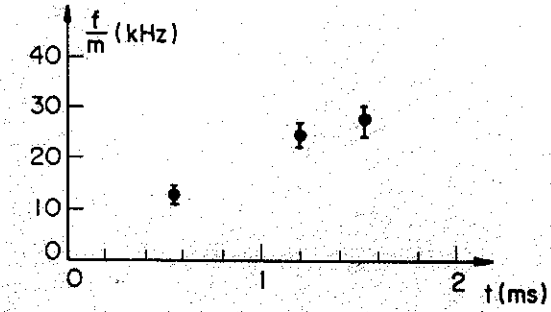

Fig. 7 - Temporal evolution of the rotation frequency of the dominant modes detected in the discharge shown in fig. 6.

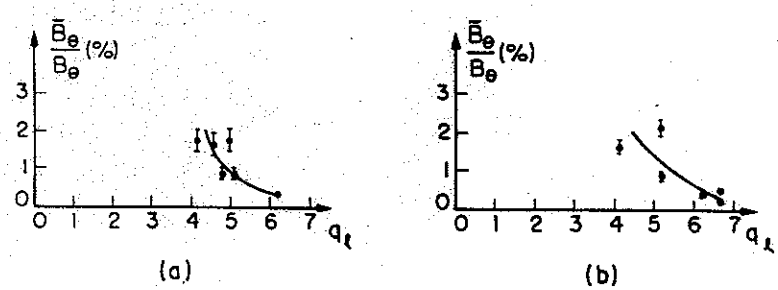

Fig. 8 - Fluctuation levels $\tilde{B}_\theta/B_\theta$ as a function of the safety factor at the limiter (q_ℓ) for (a) m=3 , n=1 and (b) m=2 , n=1 modes.